Electron-impact excitation of neutral boron using the R-matrix with pseudostates method

BALLANCE, C. P., GRIFFIN, D. C., BERRINGTON, K. A. and BADNELL, N. R.

Published version

BALLANCE, C. P., GRIFFIN, D. C., BERRINGTON, K. A. and BADNELL, N. R. (2007). Electron-impact excitation of neutral boron using the R-matrix with pseudostates method. Journal of physics B: Atomic, molecular and optical physics, 40, 1131-1139.

Electron-impact excitation of neutral boron using the R-matrix with pseudostates method

C P Ballance and D C Griffin

Department of Physics, Rollins College, Winter Park, Florida 32789

K A Berrington

School of Science and Mathematics, Sheffield Hallam University, Sheffield, S1 1WB, U.K.

N R Badnell

Department of Physics, Strathclyde University, Glasgow G1 ONG, U.K.

Abstract.

We have carried out a large R-matrix with pseudostates (RMPS) calculation of the electron-impact excitation of neutral boron. The RMPS method has been employed for the excitation/ionisation of many light fusion related species, but primarily for one or two active electrons. The present 640-term close-coupling calculation included three distinct pseudostate expansions. This enabled us to converge both the N-electron structure for three active open-shell electrons and accurately represent the high Rydberg and target continuum states. The derived Maxwell-averaged effective collision strengths will be employed to model the spectral emission from boron, which is of importance to both current (TEXTOR) and future (ITER) magnetic fusion reactors. The full set of effective collision strengths is available at the Oak Ridge National Laboratory Controlled Fusion Atomic Data Center Web site.

PACS numbers: 34.80 Kw

1. Introduction

The boronisation of the plasma exposed surfaces of tokamaks has proved to be an effective way to produce very pure fusion plasmas [1] and has been applied in tokamak experiments such as TEXTOR at Jülich and ASDEX at Garching. For progress to be made in understanding the erosion of low Z materials such as Be, B and C in the next generation of fusion experiments, transport modelling requires complete and accurate electron-impact excitation data along each of the aforementioned iosonuclear sequences. For beryllium, a complete set of non-perturbative calculations for all excitation and ionisation rates from every ion stage has already been carried out [2, 3]. In this paper, we shall consider the electron-impact excitation of neutral boron. Although Be and C are considered to be the primary candidates for plasma-facing surfaces in ITER , boron is used as a dopant for carbon in order to reduce the level of carbon chemical erosion from tokamak surfaces [4].

The data currently employed for the modelling of neutral boron within the ADAS package are derived from plane-wave Born calculations [5]. However, this simple approximation does not include any distortion of the continuum electrons nor any coupling between the bound target levels. In addition, previous RMPS calculations [6, 7, 8] have shown that the omission of the coupling of the target levels to the target continuum can lead to significantly inflated excitation cross sections above the ionisation limit, and therefore subsequent Maxwell-averaged collision strengths. An earlier study involving only hydrogenic systems [7] revealed that agreement in effective collision strengths between R-matrix and RMPS calculations was only achieved at C^{5+}, thereby suggesting RMPS calculations are required for the entire boron isonuclear sequence. The present work shall compliment the earlier RMPS calculation of Badnell *et al* [6] for singly ionised boron, and extend and improve upon the existing structure and scattering calculations of Marchalant *et al* [8] for neutral boron.

RMPS calculations have scaled dramatically with respect to computational complexity over the last few years. For example, the electron-impact excitation of near neutral hydrogenic species [7] requires only a single sequence of $nl\ ^2$L pseudostate terms, whereas helium-like systems at least double the size of the problem by involving both $1snl\ ^{1,3}L$ [28] pseudostates. The progression to electron-impact excitation of neutral beryllium [3] demands *two* configuration sequences ($2snl$ and $2pnl$), again involving both singlet and triplet terms, and a further doubling of the problem size. For all of the above pseudostate calculations, the maximum principal quantum number included was greater than or equal to 11 in order to provide the density of continuum pseudostates required to eliminate large unphysical oscillations in the cross sections above the ionisation threshold

For boron, unlike previous RMPS studies concerning only one or two active electrons outside a closed core, the present work includes three distinct ($2s^2nl$, $2s2pnl$ and $2p^2nl$) configuration expansions, two of which involve both doublet and quartet terms; all of these are necessary in order to converge both the N-electron structure and the coupling of the bound states to the target continuum. The primary difficulties in the target structure and coupling to the target continuum for B arise from the $2s2p^2$ configuration. The orbitals in this configuration have been corrected here through configuration interaction with the $2s2pnl$ and $2p^2nl$ sequences. These same pseudostate expansions also provide for coupling of $2s2p^2$ configuration with the target continuum.

The remainder of this paper is structured as follows. In the next section we outline

the RMPS method and discuss our model for neutral boron. In the results section, we compare our current findings with existing theoretical calculations, and finally in the last section, we summarise our present work and possible future directions.

2. Computational Methods

The target radial wavefunctions employed in this calculation were generated using GASP (Graphical AutoStructure Package) [9]. This is a java-based front end to the atomic structure code AUTOSTRUCTURE [10]. GASP provides an efficient and intuitive method to define hundreds of N-electron configurations, each involving many orbitals. Spectroscopic orbitals were employed for those subshells from 1s to 4f and were determined from a local potential using Slater-type orbitals. A set of non-orthogonal Laguerre pseudo orbitals was then generated from 5s to 11g; they were subsequently orthogonalised to the spectroscopic orbitals and to each other. It was determined that three distinct pseudostate expansions gave the best representation of the N-electron target and provided a sufficient density of pseudostates from the ionisation threshold to 20 eV. These N-electron target configurations are defined as follows:

- $2s^2nl$ $\quad n = 2 - 11 \;\; l = 0 - 4$
- $2s2pnl$ $\quad n = 2 - 11 \;\; l = 0 - 4$
- $2p^2nl$ $\quad n = 2 - 11 \;\; l = 0 - 3$

We have omitted the $2p^28g$, $2p^29g$, $2p^210g$, $2p^211s$, $2p^211d$ and $2p^211g$ configurations as they have minimal influence on the structure of the first 11 terms. Our goal was to provide effective collision strengths for all all transitions between the lowest eleven terms through the $2s^25s\ ^2S$ term. Configuration-interaction with the higher $2s^2ns$ pseudostates, renders the $2s^25s$ term essentially spectroscopic in terms of both energy and radiative rates. In addition, the above three pseudostate sequences lead to excellent energies for these eleven terms and ensure that all important coupling of these terms to the high-Ryderg states and the target continuua are included. The resulting 640 terms were employed in both the configuration-interaction expansion of the target and in the close-coupling expansion. Although our theoretical target energies are very close to the experimental values (see results section), due to future modelling applications of our work, they were shifted to the experimental values. Finally, AUTOSTRUCTURE was also used to generate the infinite energy Bethe/Born limits that permit interpolation of explicitly calculated RMPS results into higher temperature regimes.

The RMPS calculations were performed using our set of parallel R-matrix codes [11, 12], that are extensively modified versions of the serial RMATRIX I codes [13] that employ the pseudostate method first described in Gorczyca and Badnell 1997 [14]. The scattering calculation involved dividing the partial-wave angular momentum into three $LS\Pi$ ranges in order to minimize the size of the Hamiltonian matrices that were repeatedly diagonalised. For singlet, triplet and quintet symmetries with angular momentum in the range $L = 0 - 9$, 32 continuum basis orbitals were used to span the incident electron energy from 0 - 23 eV; for the range $L = 10 - 20$ a basis 30 orbitals was employed and in the final angular momentum range from $L = 21 - 40$ only 22 basis orbitals were required. In the final angular momentum range, the two-electron exchange integrals were not included. This is consistent with

the usual procedure of using the non-exchange codes [15] for partial-wave symmetries with angular momentum $L > 12$. The R-matrix radius was set at 70.0 Bohr radii and with over 1700 scattering channels for certain partial waves, the calculation produced large Hamiltonian matrices up to approximately 60K.

Using the parallel suite of R-matrix codes, all partial waves in each range were calculated simultaneously, and we note that those symmetries involving up to six to seven thousand $(N + 1)$-electron bound terms did not take significantly longer than those involving the largest number of scattering channels. For each partial wave, there are (nchannels*(nchannels+1)/2) continuum-continuum blocks for a particular $(N + 1)$-electron Hamiltonian matrix, and as the number of channels increases, it is the formation of these blocks that begins to dominate the computational time for the inner-region portion of the calculation.

Due to the relatively small energy separation between the first excitation threshold of 0.263 Ryds and the ionisation threshold of 0.61 Ryds, only 400 incident-electron energy mesh points were required from 0.263-0.663 Ryd to map out these slowly varying cross sections. In the energy range above the ionisation threshold, we have restricted our calculation to incident-electron energies from 0.7 Ryd to 1.5 Ryd. The maximum energy chosen is justified by the ionisation balance calculations of Mazzota *et al* [20] which show that the ionic fraction of neutral boron is negligible beyond a temperature of 6×10^4 K.

The contributions from the higher angular momentum ($L > 40$) were estimated as follows: the dipole transitions were topped-up using a method originally described by Burgess [16]; the non-dipole transitions were topped-up assuming a geometric series in L, using energy ratios, and with a special procedure to handle transitions between nearly degenerate levels based on the degenerate limiting case [17]. Any method that represents the target continuum by a finite set of L^2 basis functions will exhibit a degree of oscillation in the cross section above the ionisation threshold. We consider the calculation to be converged when these oscillations are sufficiently small that they have no appreciable impact on the Maxwell-averaged effective collision strengths.

3. Results

In table 1, we compare our present target energies with the elaborate MQDT theory calculations of Liang and Wang [23] for the $2s^2 ns, nd$ sequences and the experimental values of Odintzova and Striganov [24], reported in the NIST database [25]. We also note that the theoretical energy levels presented in [27] were transcribed incorrectly; however, subsequent correspondence with one of the authors [26] has provided the amended values given in table 1. The current calculation clearly provides improved energies over the target structure employed in this most recent RMPS scattering calculation. The average difference between our calculated energies and the experimental values [24] is 0.35%. The remaining differences could be minimized further with the inclusion of additional pseudostates with higher principal quantum numbers; however, the slight additional improvements in the target structure that would be achieved are far outweighed by the computational cost of an even larger scattering calculation.

In table 2, we present a selection of the strongest dipole-allowed oscillator strengths from the groundstate and the $(2s^2 3p)^2 P$ excited term; We note the almost unitary length to velocity ratios of the present calculation. They are improved over the oscillator strength length to velocity ratios for the n=3 terms obtained by Marchant *et*

al [8], which are also given in this table. For transitions involving the n=4 terms, only the weak $(2s^2 3p)^2P \rightarrow (2s^2 4d)^2D$ transition has a length to velocity ratio appreciably different from 1.0. The radiative rates available in the NIST database [25] are not included in this comparison as they are classified with an accuracy rating of C or less.

There are 55 possible transitions amongst the first 11 spectroscopic terms; the six transitions discussed below provide a representative sample of these excitations. Figure 1 was chosen in order to show the level of agreement between the present calculation and the previous RMPS calculation for transitions between $n = 2$ terms. Figures 2 and 3 highlight the improved convergence of our calculations over previous work for transitions to the n=3 terms from the ground and metastable terms. In figure 4, we show transitions involving the $n = 4$ terms that have not been included in the earlier RMPS calculation. Finally in figure 5, we consider a near-degenerate dipole transition, which is insensitive to the effects of continuum coupling.

As illustrated in figure 1, there is excellent agreement with the earlier RMPS calculation for the transition from the groundstate to the $(2s2p^2)^4P$ term . This spin-forbidden transition has the largest peak cross section in the low energy region, and should strongly populate the metastable term at low temperatures. It is only beyond 0.5 Ryd, that the groundstate to $(2s2p^2)^2D$ cross section begins to have a comparable magnitude. Also incorporated within figure 1 is the energy distribution of those pseudostates that are above the ionisation threshold, grouped according to their term angular momentum. A significant number of pseudostates lie above 20 eV, but as explained previously [20], we have not pursued scattering calculations in this energy range.

Figure 2 shows the electron-impact excitation cross section for the dipole-allowed transition $(2s^2 2p)^2P - (2s^2 3s)^2S$. Above the ionisation threshold the almost flat cross section obtained from the present calculation does not exhibit any of the large pseudoresonances evident in the earlier RMPS calculation [8]; this clearly illustrates the high level of convergence of the present pseudostate expansion.

In figure 3, we show the two-electron excitation from the metastable $(2s2p^2)^4P$ to the $(2s^2 3d)^2D$ term. At energies above about twice the ionisation threshold there is excellent agreement with results from the earlier RMPS results [27]. However, in the low-energy region, the pseudoresonances that straddle the ionisation threshold in the earlier work are probably due to a lack of convergence in the 2s2pnl expansion. Large unphysical resonances like these close to an excitation threshold have a large impact on low temperature effective collision strengths. We note that in order to make this comparison, we had to shift the energy scale used in figure 3 of reference [27] so that it is relative to the ^4P metastable term, rather than the groundstate.

The RMPS cross sections for transitions from the groundstate to higher n shells in neutral atomic systems will exhibit more pseudoresonance structure as the magnitude of the background cross section weakens. It has been shown in previous work on helium [28] and beryllium [3] that for excitations from the groundstate to high n shells close to the ionisation theshold, there are differences of a factor of two or more between RMPS and standard R-matrix cross sections due to coupling to the target continuum. In figure 4, we show the cross sections for the dipole-allowed transitions from the groundstate to the higher $(2s^2 4s)^2S$ and $(2s^2 4d)^2D$ terms. We would expect standard R-matrix calculations for boron to overestimate the cross section by a similar magnitude; therefore, the small undulations at 0.75 Ryds in our present calculation are acceptable in light of the large correction obtained from the use of these pseudostates to represent the continuum coupling.

In figure 5, we show the cross section for the strong dipole excitation $(2s^2 3p)^2P - (2s^2 3d)^2D$. The low angular momentum partial waves couple both of these terms to the target continuum; however, because of the small excitation energy, the cross section for this transition is dominated by contributions from partial waves with high angular momentum. Thus the effects of continuum coupling for such excitations are quite small (see Ballance *et al* [32]). Above the energy for ionisation from the $(2s^2 3p)^2P$ term of 0.167 Ryd, there are some small oscillations; however, for such a large cross section their effect on the Maxwell-averaged effective collision strengths is completely negligible.

We can conclude from these representative figures that, in comparison to earlier RMPS studies [8, 27], this calculation benefits significantly from the approximately 600 pseudostates that have been included above the ionisation threshold. Cross sections involving transitions from the groundstate to the $n = 2$ and $n = 3$ terms are much more fully converged, and we also expect highly accurate results for excitation to the $n = 4$ terms.

The full set of results for energy levels, dipole radiative rates and effective collision strengths (including Born/Bethe limits) for the first 10 terms over $T = 1 \times 10^4 - 2 \times 10^5$ K, tabulated in the ADAS *adf04* format (Summers 1999) [22], is available via the WWW at http://www-cfadc.phy.ornl.gov/data_and_codes.

4. Summary

Both highly accurate atomic structure and electron-impact excitation calculations for neutral boron have been made, which both improve and extend past work. The large pseudostate expansion brings both the target and scattering calculation to a higher levels of convergence than previously obtained.

Excitation rates for all ionisation stages of boron are required in order to generate the generalised collisional radiative (GCR) coefficients [30] needed for the modelling of a plasma containing boron. With this calculation for the neutral species, RMPS results for electron-impact excitation are now available for every ionisation stage. Results for B^+ [6] and B^{4+} [7] have been published previously. The unpublished results for B^{2+} and B^{3+} are now available. For B^{3+} the calculation follows the outline given in reference [31] and the B^{2+} calculation is similar to that used for He-like Be given in reference [3]. All these RMPS results will be archived in the form of Maxwell-averaged effective collision strengths both at Oak Ridge [33] and within the ADAS package [22].

Although we have considered only electron-impact excitation here, a similar calculation will also enable us to determine highly accurate ionisation cross sections from the ground and metastable states of boron. Only the $2s^2 nl$ and $2s2p nl$ sequences would be required for groundstate ionisation, whereas the metastable $(2s2p^2)^4P$ ionisation also requires the $2p^2 nl$ sequence. This will be considered in future work.

Acknowledgments

This work was supported in part by grants from the US Department of Energy. Computational work was carried out at the National Energy Research Scientific Computing Center in Oakland, California and at the National Center for Computational Sciences in Oak Ridge, Tennessee. CPB and DCG, would like to recognize the contribution of the summer undergraduate research program at Rollins College, and in particular, the efforts of Ms. Jeanmarie Loria and Mr. Erich Blossey

in developing the GASP package. CPB would also like to acknowledge the application G3DATA written by Carl Frantz that was used in the preparation of this document.

References

[1] Winter J, Grobusch L, Rose T, Seggern J von, Esser H G and Wienhold P 1992 *Plasma Sources Sci. Technol* **1** 82
[2] Colgan J, Loch S D, Pindzola M S, Ballance C P and Griffin D C 2003 *Phys. Rev. A* **68** 032712
[3] Ballance C P, Griffin D C, Colgan J, Loch S D and Pindzola M S 2003 *Phys. Rev. A* **68** 062705
[4] Davis J W and Haasz A A 1997 *Journal of Nuclear Materials* **241-243** 37
[5] O'Mullane 2006 *private communication*
[6] Badnell N R, Griffin D C and Mitnik D M 2003 *J. Phys. B: At. Mol. Opt. Phys.* **36** 1337
[7] Ballance C P, Badnell N R and Smyth E 2003 *J. Phys. B: At. Mol. Opt. Phys.* **36** 3707
[8] Marchalant P J, Bartschat K, Berrington K A and Nakazaki S 1997 *J. Phys. B: At. Mol. Opt. Phys.* **30**, L279
[9] http:://vanadium.rollins.edu/GASP.html
[10] Badnell N R 1997 *J. Phys. B: At. Mol. Opt. Phys.* **30** 1
[11] Mitnik D M, Griffin D C, Ballance C P, and Badnell N R 2003 *J. Phys. B: At. Mol. Opt. Phys.* **36** 717
[12] Ballance C P and Griffin D C 2004 *J. Phys. B: At. Mol. Opt. Phys.* **37** 2943
[13] Berrington K A, Eissner W B and Norrington P H 1995 *Comp. Phys. Commun.* **92** 290
[14] Gorczyca T W and Badnell N R 1997 *J. Phys. B: At. Mol. Opt. Phys.* **30** No 8 2011
[15] V M, Burke P G and Scott N S 1992 *Comp. Phys. Commun.* **69** 76
[16] Burgess A, 1970 *J. Phys. B: At. Mol. Opt. Phys.* **7**, L364.
[17] Burgess A, Hummer D G, and Tully J A 1974 *Phil Trans. R. Soc. A* **266**, 225
[18] Gorczyca T W, Robicheaux F, Pindzola M S, Griffin D C and Badnell N R 1995 *Phys. Rev. A* **52** 3877
[19] Ballance CP and Griffin D C 2004 *J. Phys. B: At. Mol. Opt. Phys.* **37** No 14 2943
[20] Mazzotta P, Mazzitelli G, Colafrancesco S and Vittorio N 1998 *Astron. Astrophys. Suppl. Ser.* **133** 403
[21] Kim Y and Stone P M 2001 *Phys. Rev. A* **64** 052707
[22] Summers H P *ADAS User Manual Version 2.9* webpage 2005 http://adas.phys.strath.ac.uk
[23] Liang L and Wang Y C 2003 *J. Phys. B: At. Mol. Opt. Phys.* **36** 4387
[24] Odintzova G A and Striganov A R 1979 *J. Phys. Chem. Ref. Data* **8** 63
[25] http:://physics.nist.gov
[26] Bartschat K 2006 *private communication*
[27] Marchalant P J and Bartschat K 1997 *J. Phys. B: At. Mol. Opt. Phys.* **30**, 4373
[28] Ballance C P, Griffin D C, Badnell N R, Loch S D and M S Pindzola 2004 "Atomic Process in Plasmas 14th APS Topical Conference on Atomic Processes in Plasmas" p. 25 ISBN 0-7354-0211-6 , Ed. James S. Cohen, Stephane Mazevet and David P. Kilcreases.
[29] Griffin D C, Pindzola M S, Gorczyca T W, and Badnell N R 1995 *Phys. Rev. A* **51** 2265
[30] Summers H P, Dickson W J, OMullane M G, Badnell N R, Whiteford A D, Brooks D H, Lang J, Loch S D and Griffin D C 2005 *Plasma Phys. and Controlled Fusion* **48** 263
[31] Griffin D C, Badnell N R and Pindzola M S 1999 *J. Phys. B: At. Mol. Opt. Phys.* **32** No 17 L479
[32] Ballance C P, Griffin D C, Loch S D, Bovin R F and Pindzola M S 2006 *Phys. Rev. A* **74** 012719
[33] http://www-cfadc.phy.ornl.gov/data_and_codes

Table 1. Energies of the first 11 terms of B I relative to the $(2s^22p)^2P$ groundstate. All energies are in Rydbergs. Experimental values refer to the NIST database, but based upon the experimental work of Odintzova and Strignov . The theoretical results are from Liang and Wang † and Bartschat ‡.

No.	Config.	term	energy present	energy theory‡	energy theory†	energy expt.
1	$2s^22p$	^2p	0.000	0.000	0.000	0.000
2	$2s2p^2$	^4P	0.261	0.256	-	0.263
3	$2s^23s$	^2S	0.367	0.372	0.365	0.365
4	$2s2p^2$	^2D	0.441	0.448	-	0.436
5	$2s^23p$	^2P	0.442	0.461	-	0.443
6	$2s^23d$	^2D	0.499	0.517	0.499	0.499
7	$2s^24s$	^2S	0.501	-	0.501	0.501
8	$2s^24p$	^2P	0.525	-	-	0.527
9	$2s^24d$	^2D	0.545	-	0.547	0.547
10	$2s^24f$	^2F	0.545	-	-	0.547
11	$2s^25s$	^2S	0.549	-	0.548	0.548

Table 2. Oscillator strengths from the groundstate and $(2s^23p)^2P$ term. The present work is compared with the theoretical values of Marchalant *et al*

Transition	present (length)	ratio (l/v)	Marchalant *et al* (length)	Marchalant *et al* ratio (l/v)
$(2s^22p)^2P \rightarrow (2s^23s)^2S$	0.07334	0.99	0.07972	1.02
$(2s^22p)^2P \rightarrow (2s^23d)^2D$	0.01648	1.02	0.17870	1.16
$(2s^22p)^2P \rightarrow (2s^24s)^2S$	0.01245	1.05	-	-
$(2s^22p)^2P \rightarrow (2s^24d)^2D$	0.07240	1.05	-	-
$(2s^23p)^2P \rightarrow (2s^23s)^2S$	1.07300	1.02	1.21210	1.27
$(2s^23p)^2P \rightarrow (2s^23d)^2D$	0.85259	0.99	0.87760	1.03
$(2s^23p)^2P \rightarrow (2s^24s)^2S$	0.19222	1.04	-	-
$(2s^23p)^2P \rightarrow (2s^24d)^2D$	0.00048	0.78	-	-

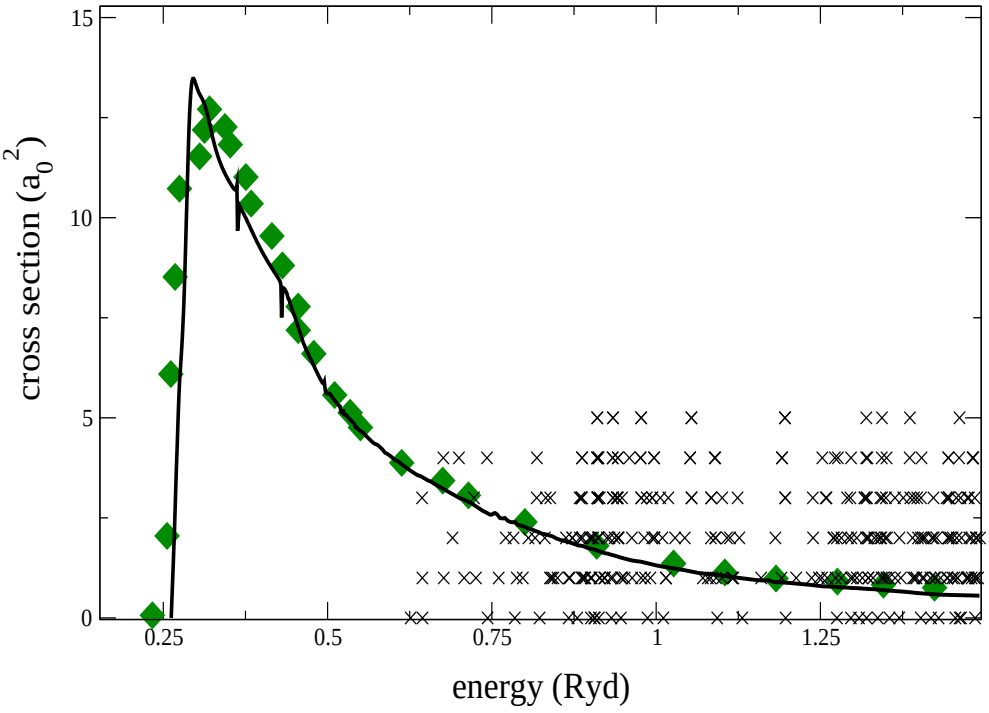

Figure 1. Cross section for the $(2s^2 2p)^2P$ to $(2s2p^2)^4P$ transition, in units of a_O^2. Diamonds : Marchalant *et al* [8]; solid: present calculation. The crosses represent the distribution of pseudostates above the ionisation threshold, with the y axis defining the angular momentum of the individual pseudostate terms

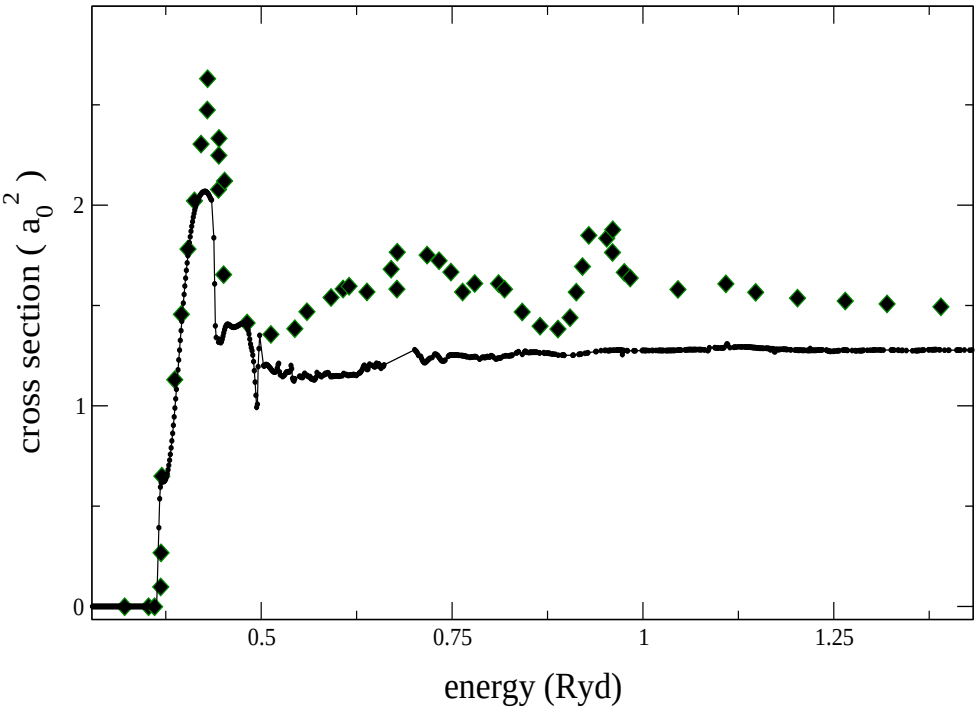

Figure 2. Cross section of the $(2s^2 2p)^2P$ to $(2s^2 3s)^2S$ transition, in units of a_O^2. Diamonds: Marchalant *et al* [8]; solid: present calculation.

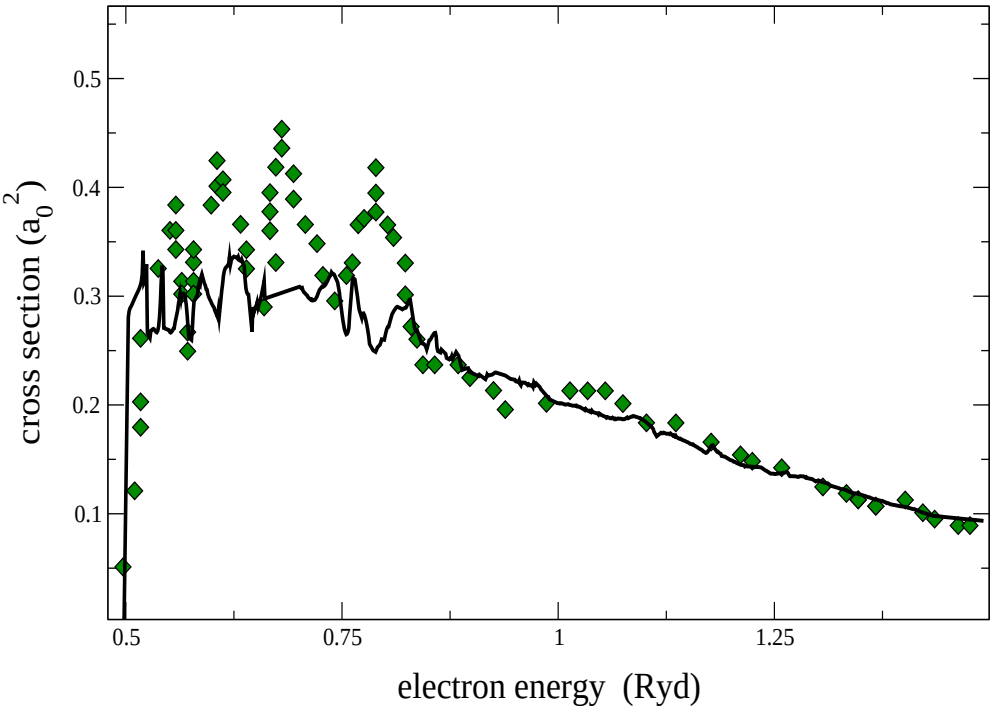

Figure 3. Cross section of the $(2s2p^2)^4P$ to $(2s^23d)^2D$ transition, in units of a_O^2. Diamonds: Marchalant *et al* [8]; solid: present calculation.

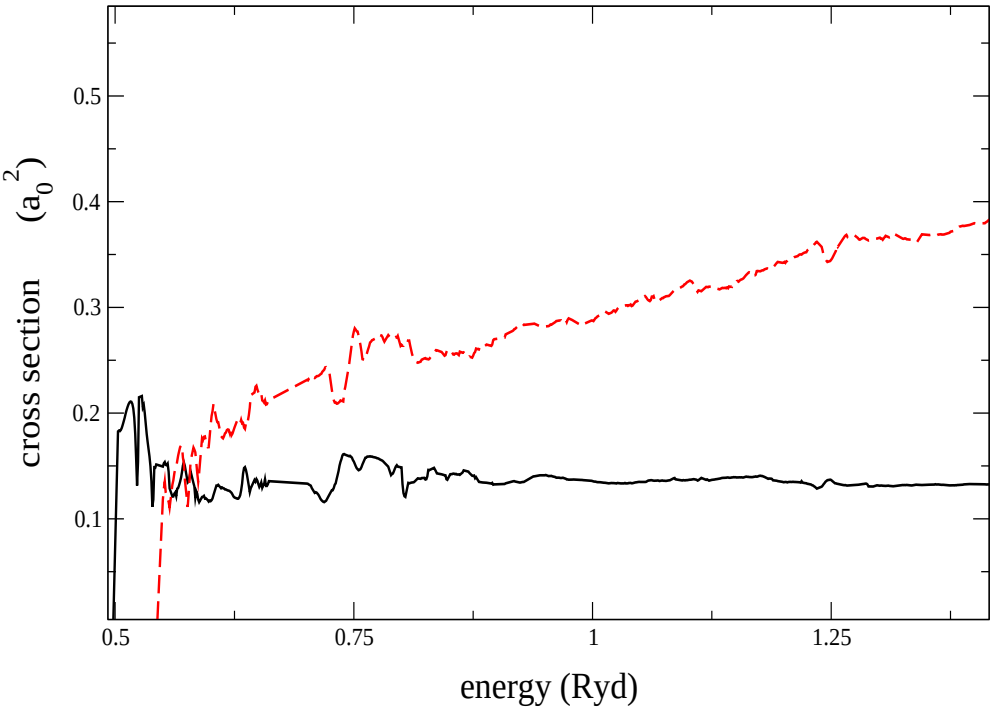

Figure 4. Cross section for excitation from $(2s^2 2p)^2P$ to both the $(2s^2 4s)^2S$ and $(2s^2 4d)^2D$ terms in units of a_O^2. solid: 4s; dashed: 4d.

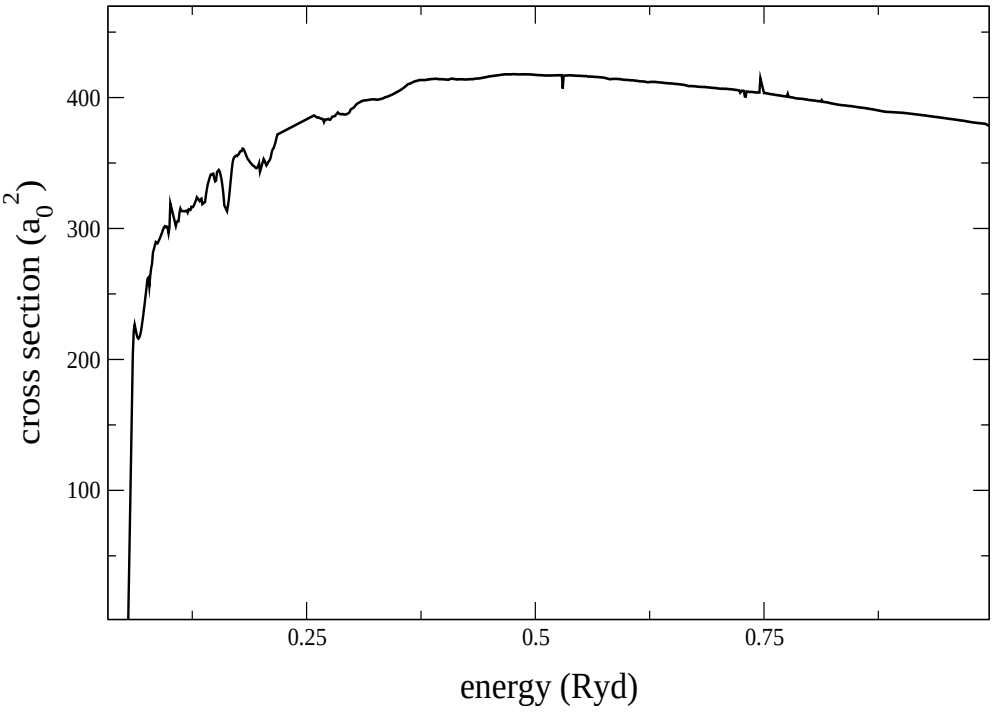

Figure 5. Cross section of the near degenerate dipole allowed $(2s^2 3p)^2P$ - $(2s^2 3d)^2D$ transition in units of a_O^2.